Overexpression of long non-coding RNA SBF2-AS1 promotes cell progression in esophageal squamous cell carcinoma (ESCC) by repressing miR-494 to up-regulate PFN2 expression

Qiu Zhang[#,1], Xixiang Pan[#,1], Dongyang You[*,1]

[1]Oncology Department of Thoracic Head and Neck Surgical, Huangshi Central Hospital (Affiliated Hospital of Hubei Polytechnic University), Edong Healthcare Group, Huangshi, Hubei, China

[#]Qiu Zhang and Xixiang Pan contributed equally to this work.

[*]**Corresponding author:** Dongyang You, Oncology Department of thoracic head and neck surgical, Huangshi Central Hospital (Affiliated Hospital of Hubei Polytechnic University), Edong Healthcare Group, No. 293, Yiyuan Street, Huangshi, 435000, Hubei, China

E-mail: zuibizhi19821@126.com   Tel.: 86-0714-3189999

ABSTRACT

Esophageal squamous cell carcinoma (ESCC) is an intractable esophageal cancer caused by smoking, alcohol consumption and nutritional deficiencies. Recently, long non-coding RNA SET-binding factor 2 antisense RNA 1 (SBF2-AS1) was validated as an oncogene in multiple cancers. However, the mechanism of SBF2-AS1 in ESCC progression is poorly understood. In the present research, we found that the expression of SBF2-AS1 and PFN2 was up-regulated, while miR-494 was down-regulated in ESCC tumors and cells using quantitative real-time polymerase chain reaction (qRT-PCR). 3-(4, 5-dimethyl-2-thiazolyl)-2, 5-diphenyl-2-H-tetrazolium bromide (MTT) assay and transwell assay demonstrated that silencing of SBF2-AS1 suppressed proliferation, migration and invasion. Moreover, western blot showed that SBF2-AS1 deletion also inhibited epithelial to mesenchymal transition (EMT) by detecting MMP9, Vimentin and E-cadherin protein expression. We confirmed that miR-494 was a target of SBF2-AS1 by luciferase reporter system, RIP and RNA pull-down assay. In addition, miR-494 inhibitor reversed the repression induced by SBF2-AS1 silencing on ESCC cell proliferation, migration, invasion and EMT. Furthermore, PFN2 was negatively regulated by miR-494. Besides, restoration of PFN2 inversed the inhibition effects on cell proliferation, migration, invasion and EMT induced by SBF2-AS1 silencing in ESCC. In conclusion, SBF2-AS1 contributed to cell proliferation, migration, invasion and EMT in ESCC by enhancing PFN2 expression via sponging miR-494, providing promising biomarkers for ESCC diagnosis and treatment.

Keywords: SBF2-AS1, miR-494, PFN2, progression, ESCC

INTRODUCTION

Esophageal squamous cell carcinoma (ESCC) which originated from esophageal epithelial cells, accounts for over 90% esophageal cancers (Hou et al., 2018; Kang et al., 2018). The major pathogenic factors include smoking, alcohol consumption and nutritional deficiencies (Guo et al., 2018). Despite advanced interventions, such as optimal surgery followed by chemotherapy, the 5-year survival rate is approximately 15% since distant metastasis, high aggressiveness and locoregional recurrence (Kawaguchi et al., 2017; Nishiumi et al., 2019; Wu, Yang, & Xian, 2019). Therefore, illumination of the underlying pathogenesis of ESCC is urgently needed.

Long noncoding RNAs (lncRNAs) are conserved transcripts that functionally participate in cell regulation of many diseases, especially cancers (L. Chen et al., 2019; Hong, Chen, Wu, & Wang, 2018; X. Hu, Ding, Zhang, & Cui, 2019). LncRNA SET-binding factor 2 antisense RNA 1 (SBF2-AS1) mapped on human chromosome 11p15.1, was a newly identified oncogene in multiple cancers, such as small-cell lung cancer, cervical and colorectal cancer (Y. Zhang, Li, Han, Zhang, & Sun, 2019). As competing endogenous RNA (ceRNA), SBF2-AS1 accelerated cell progression in acute myeloid leukemia by targeting miR-188-5p (Y. J. Tian et al., 2019). Moreover, overexpression of SBF2-AS1 enhanced cell proliferation and invasion in colorectal cancer by sponging miR-619-5p to up-regulate HDAC3 expression (G. Chen et al., 2019). Chen and his colleagues reported that SBF2-AS1 upregulation was observed in ESCC (Chen et al., 2018). LncBase Predicted v.2 predicted that microRNA-494 (miR-494) was a target gene of SBF2-AS1. MiR-494, a small chain noncoding RNA, was demonstrated to function as tumor promoter or suppressor in tumorigenesis and progression

in cancers (J. Zhang et al., 2019; Cheng et al., 2018; N. Li et al., 2016). However, the functional role and the regulatory mechanism of SBF2-AS1/miR-494 axis were still unknown.

Profilin 2 (PFN2) is a member of profiling family that exclusively expressed in the central nervous system. PFN2 was also closely related to cell proliferation and migration in a variety of cancers (Jeong, Choi, Seo, Lee, & Yoo, 2018). In addition, PFN2 was recognized as essential unfavorable prognosis biomarker of different cancers, including ESCC (Cui et al., 2016). Therefore, the function of PFN2 in ESCC requires in-depth exploration.

We aimed to illuminate the regulatory effects of SBF2-AS1 on ESCC cell progression. The expression of SBF2-AS1, miR-494 and PFN2 was evaluated. Moreover, loss-of-function experiment was conducted to explore the effects of SBF2-AS1 on cell proliferation, migration, invasion and EMT of ESCC cells. Besides, the influence of SBF2-AS1/miR-494/PFN2 axis on cell behavior of ESCC cells was also investigated.

MATERIALS AND METHODS

Tissue samples

ESCC patients (n=50) were recruited from Huangshi Central Hospital (Affiliated Hospital of Hubei Polytechnic University). All the patients were informed and signed informed consent. ESCC tumor tissues (n=50) and normal tissues (n=15) were obtained from those patients by surgery and subjected to the following experiments. Our protocols were approved by Ethics Committee of Huangshi Central Hospital (Affiliated Hospital of Hubei Polytechnic University).

Cell culture and transfection

Eca-109, KYSE-150, TE-1 cells were purchased from Chinese Academy of Sciences (Shanghai, China), KYSE-140 cells were purchased from Bioleaf (Shanghai, China) and human esophageal epithelium immortalized cells HET-1A were purchased from American Type Culture Collection (ATCC, Manassas, VA, USA). All the cells were maintained in DMEM medium (Gibco, Carlsbad, CA, USA) supplemented with 10% FBS (Gibco) and 0.05% penicillin/streptomycin.

PFN2 overexpression vector was obtained by cloning the sequences of PFN2 (423 bp, GeneBank accession No. KM517577) (Genepharma, Shanghai, China) into pcDNA3.1 (Invitrogen, Carlsbad, CA, USA), termed pcDNA3.1-PFN2 (PFN2). Before transfection, Eca-109 and KYSE-150 cells (4×10^5 cells per well) were seeded into 12-well plate. After incubation for 24 h, 0.2 μg of PFN2 overexpression vector (PFN2) were transfected into Eca-109 and KYSE-150 cells using 0.5 μL of Lipofectamine 2000 reagent (Invitrogen). Moreover, those oligonucleotides included that small harboring RNA (shRNA) targeting SBF2-AS1 (2,708 bp, GeneBank accession No. NR_036485) (sh-SBF2-AS1) and the negative control (sh-NC) were synthesized by Genepharma (Shanghai, China), and miR-494 mimics and negative control (miR-NC) were purchased from RIBOBIO (Guangzhou, China). Eca-109 and KYSE-150 cells were transfected with 0.5 μg of aforementioned oligonucleotides using 0.6 μL of Lipofectamine 2000 (Invitrogen). After transfection for 48 h, the transfected cells were used for further analysis.

Quantitative real-time polymerase chain reaction (qRT-PCR)

QRT-PCR was performed following the method described in our earlier study (Y. J. Tian et al., 2019). Total RNA was obtained by incubating ESCC tissues and cells with TRIzol reagent (Invitrogen). Then, a NaniDrop ND-1000 Spectrophotometer (NaniDrop, Wilmington, MA, USA) was used to quantify RNA, and its purity was detected using the A260/280 ratio. Reversely transcription assay (5 μg RNA) was carried out to synthesize cDNA by All-in-One™ First-Strand cDNA Synthesis Kit (FulenGen, Guangzhou, China). Briefly, the transcription was conducted in a 10 μL reaction mixture, including polyadenylated RNA (100 ng), 5 × PrimeScript Buffer (2 μL), PrimeScript RT Enzyme Mix I (0.5 μL), RT primer mixure (1 μL), and RNase-free water. Whereafter, total reaction mixture was incubated at 50˚C for 15 min and 85˚C for 5 sec. Then, qRT-PCR was performed using SYBR green (Applied Biosystems, Foster City, CA, USA) in 15 μL final volumes containing 1.5 μL template cDNA mixed with 7.5 μL 2 ×SYBR Green PCR master mix and 3 μL of each forward and reverse primers. GAPDH and U6 were exploited as internal reference. The relative expression of HOXA10 and miR-128/miR-142 was calculated using $2^{-\Delta\Delta Ct}$ method. The amplification parameters were as follows: denaturation at 95˚C for 10 min, followed by 40 cycles of denaturation at 95˚C for 30s, annealing at 60˚C for 30s and extension at 72˚C for 1min. The primers for SBF2-AS1, miR-494, PFN2 GAPDH, and U6 were listed in Table S1. The fold changes of individual genes were detected by $2^{-\Delta\Delta Ct}$ methods (VanGuilder, Vrana, & Freeman, 2008).

3-(4, 5)-dimethylthiazole-2-y1)-2, 5-biphenyl tetrazolium bromide (MTT)

Transfected Eca-109 and KYSE-150 cells (5×10^4 cells per well) were inoculated on 96-well plates and incubated for 24 h, 48 h and 72 h. Then, 10 μL MTT (Beyotime, Shanghai, China) was added to each well at the different time points (0 h, 24 h, 48 h, 72 h) for 4 h at 37°C, followed by incubating with 100 μL dimethyl sulfoxide (DMSO; Sangon, Shanghai, China) for 2 h. Finally, the OD value (490 nm) was measured by a spectrophotometer (Xia et al., 2020).

Transwell assay

Cell migration and invasion were determined using Transwell chambers (24-well, Sigma-Aldrich). The upper chamber of transwell was treated with Matrigel (without Matrigel coating for migration assay). In briefly, transfected Eca-109 and KYSE-150 cells (7×10^4 cells per well) were resuspended in serum-free DMEM (Gibco). Then, the medium containing the cells were seeded into the upper chamber. Meanwhile, the lower chamber was supplemented with the medium containing 10% FBS (Gibco) as chemoattractant. After incubation for 48 h, the non-migrated and non-invasive cells were scraped, while the migrated and invaded cells at the lower chamber of transwell were fixed with methsnol and stained with 0.1% crystal violet (Sigma, St. Louis, MO, USA). The number of migrated and invaded cells was counted using a microscope (Lv et al., 2016).

Western blot assay

PFN2, N-cadherin, Vimentin and E-cadherin protein were isolated from transfected Eca-109

and KYSE-150 cells using pre-cold RIPA buffer reagent (Thermo Fisher Scientific, Waltham, MA, USA) containing protease inhibitor (Cocktail, Roche, Basel, Switzerland). Then, a Bicinchonnic Acid Protein Assay kit (Thermo Fisher Scientific) was used to detect the protein concentration. 20 μg proteins were separated by 10% sodium dodecyl sulphate-polyacrylamide gel electrophoresis (SDS-PAGE), transferred to polyvinylidene difluoride membranes (Millipore, Billerica, MA, USA) and blocked by 5% nonfat milk at room temperature for 1.5 h. Then, the membranes were incubated with primary antibodies against PFN2 (1:1000 dilution, ab230673, Abcam, Cambridge, MA, USA), N-cadherin (1:1000 dilution, ab18230, Abcam), Vimentin (1:1000 dilution, ab18230, Abcam) and E-cadherin (1:1000 dilution, ab76055, Abcam) overnight at 4°C, followed by incubating with HRP-conjugated secondary antibody (Sangon) for 1 h at 37°C. Finally, the protein signals were determined using an electrochemiluminescent system (PerkinElmer Life Science, Waltham, MA, USA) (Wang et al., 2010).

Subcellular localization

The localization of SBF2-AS1 was detected by cytoplasmic & Nuclear RNA Purification Kit (Norgen Biotek Corp., Belmont, MA, USA). Briefly, cells were lysed and then centrifugated. Subsequently, the cytoplasmic RNA and nuclear RNA were incubated with Buffer SK and anhydrous ethanol, respectively. Then, the nuclear RNA and cytoplasmic RNA were eluted using the spin column. Finally, the expression of SBF2-AS1 in cytoplasmic and nucleus fractions was detected by qRT-PCR (Zhou et al., 2019).

Luciferase reporter assay

LncBase Predicted v.2 predicted that miR-494 was a target gene of SBF2-AS1 and starBase 2.0 predicted that PFN2 was a target gene of miR-494. Based on these prediction results, SBF2-AS1 sequence (2,708 bp, GeneBank accession No. NR_036485) or PFN2 3'UTR sequence (423 bp, GeneBank accession No. KM517577) containing wide-type or mutant-type miR-494 (location: chr14, 101029681-101029702. putative binding sequence: AUACAAAG or ACAAAG) targeting sites were cloned into pmirGLO vector (Promega, Madison, Wisconsin, USA), termed WT-SBF2-AS1 or MUT-SBF2-AS1, and PFN2 3'UTR-WT or PFN2 3'UTR-MUT reporter plasmids. Wild type (WT-SBF2-AS1, PFN2 3'UTR-WT) and mutant type (MUT-SBF2-AS1, PFN2 3'UTR-MUT) luciferase vectors were constructed. DNA sequencing was used to detect the reporters. Then, 400 ng of the constructed plasmids, 50 ng of renilla luciferase reporter plasmid (pRL-TK) and 50 nM of miR-NC and miR-494 were transfected into Eca-109 and KYSE-150 cells using Lipofectamine 3000 (Invitrogen). After 48 h incubation, a Microplate reader (Biotek Instruments) and dual luciferase reporter assays kit (Promega) were used to determine the relative luciferase activity. Renilla luciferase activity was regarded as the internal control for the normalization of firefly luciferase activity (X. Rong et al., 2019).

RNA immunoprecipitation (RIP) assay

RIP assay was carried out using RIP™ RNA-Binding Protein Immunoprecipitation Kit (Millipore) (Wu et al., 2019). Firstly, 2×10^5 Eca-109 and KYSE-150 cells were lysed by RIP buffer. Then, the cell lysis was incubated with magnetic beads coated with Anti-Ago2 or

Anti-IgG antibody (Millipore). The enrichment of SBF2-AS1 was analyzed by qRT-PCR.

RNA pull-down assay

A pull-down assay was performed as previously described (Gao et al., 2019). Briefly, 2×10^5 Eca-109 and KYSE-150 cells were collected, lysed, and sonicated. Biotinylated wild type miR-494 (Bio-miR-494-WT), mutant type miR-494 (Bio-miR-494-MUT) and negative control (Bio-NC) synthesized by RiboBio (Guangzhou, China) were transfected into Eca-109 and KYSE-150 cells. Then, Eca-109 and KYSE-150 cells were incubated with Dynabeads M-280 Streptavidin (Invitrogen) for 10 min. After washing with wash buffer, the RNA complexes bound to the beads were eluted and isolated using the RNeasy Mini Kit (QIAGEN) for RT-PCR.

Statistical analysis

Data were presented as means ± standard deviation (SD). Statistical analysis was performed by GraphPad Prism 7. The survival curve was plotted by Kaplan-Meier analysis. Paired Student's *t*-test or one-way analysis of variance (ANOVA) was exploited to compare two or more samples. The correlation between miR-494 and SBF2-AS1 or PFN2 was analyzed by Pearson's correlation coefficient. *P* value less than 0.05 (*P*<0.05) was considered statistically significant.

RESULTS

SBF2-AS1 was closely associated with poor prognosis of ESCC

Initially, the role of SBF2-AS was evaluated by measuring the expression of SBF2-AS using GEPIA2 (http://gepia2.cancer-pku.cn/#index) and qRT-PCR. As displayed in Fig. 1A-B, SBF2-AS expression was up-regulated in ESCC tumors compared with normal tissues. Meanwhile, SBF2-AS level was considerably higher in ESCC cell lines (TE-1, KYSE-140, KYSE-150, Eca-109) than that of human esophageal epithelium immortalized cells HET-1A (Fig. 1D). Moreover, the survival rate was significantly reduced in ESCC patients with high SBF2-AS level. By contrast, low SBF2-AS level resulted in relatively high survival rate (Fig. 1C). Hence, overexpression of SBF2-AS contributed to poor prognosis of ESCC.

Depletion of SBF2-AS1 repressed cell proliferation, migration, invasion and EMT in ESCC

Functionally depletion of SBF2-AS1 was conducted to further explore the influence of SBF2-AS1 on proliferation, migration, invasion and EMT of ESCC cells. It was apparent that SBF2-AS1 expression was distinctly decreased in Eca-109 and KYSE-150 cells stably transfected with sh-SBF2-AS1 compared with sh-NC group, indicating that the transfection efficiency was extremely high (Fig. 2A). Cell proliferation was repressed by SBF2-AS1 silencing (Fig. 2B-C). Meanwhile, SBF2-AS1 silencing evidently attenuated cell migration and invasion of ESCC cells (Fig. 2D-E). In addition, the expression of EMT associated protein MMP9, Vimentin and E-cadherin was analyzed by western blot. As illustrated in Fig. 2F, the expression of MMP9, Vimentin was reduced whereas E-cadherin expression was

boosted, demonstrating that SBF2-AS1 knockdown restricted EMT process. Collectively, depletion of SBF2-AS1 inhibited cell proliferation, migration, invasion and EMT in ESCC.

SBF2-AS1 acted as sponge of miR-494

The interaction between SBF2-AS1 and miR-494 was further determined by qRT-PCR and luciferase reporter system. Obviously, SBF2-AS1 was highly expressed in the cytoplasm of Eca-109 and KYSE-150 cells in comparison with nuclear, clarifying that SBF2-AS1 mainly exerted its function in the cytoplasm of cells (Fig. 3A-B). Bioinformatics analysis by LncBase Predicted v.2 showed the existence of putative binding sites between SBF2-AS1 and miR-494 (Fig. 3C). In addition, down-regulation of miR-494 expression was observed in ESCC tumors and cells compared with the matched normal ones (Fig. 3D-E). There was also a negative linear relation between expression of SBF2-AS1 and miR-494 (r=-0.67, *P*<0.001) (Fig. 3F). What's more, miR-494 expression in ESCC cells was enhanced by miR-494 transfection (Fig. 3G). Reduction of luciferase activity in Eca-109 and KYSE-150 cells co-transfected with WT-SBF2-AS1 and miR-494 validated the interaction between SBF2-AS1 and miR-494 (Fig. 3H-I). As expected, RIP assay showed that the enrichment of SBF2-AS1 was up-regulated in ESCC cells incubated with Anti-Ago2 compared with Anti-IgG (Fig. 3J). By contrast, the enrichment of SBF2-AS1 was distinctly enhanced by Bio-miR-494-WT compared with Bio-miR-494-MUT (Fig. 3K). Meanwhile, SBF2-AS1 silencing facilitated the expression of miR-494 in ESCC cells, suggesting SBF2-AS1 could regulate the expression of miR-494 (Fig. 3L). Taken together, SBF2-AS1 was a sponge of miR-494.

MiR-494 inhibitor restrained SBF2-AS1 silencing-induced suppression on cell proliferation, migration, invasion and EMT in ESCC

The regulatory effects of SBF2-AS1/miR-494 axis on ESCC progression were assessed. Apparently, miR-494 expression was enhanced by SBF2-AS1 knockdown while reduced by miR-494 inhibitor (Fig. 4A). As exhibited in Fig. 4B-C, miR-494 inhibitor obviously rescued SBF2-AS1 silencing-induced inhibition of cell growth. Consistently, miR-494 inhibitor counteracted SBF2-AS1 silencing-mediated repression on ESCC cell migration and invasion (Fig. 4D-E). Besides, the expression of protein MMP9 and Vimentin was blocked by SBF2-AS1 silencing. However, the blockage was inversed by miR-494 inhibitor. By comparison, the expression of protein E-cadherin exhibited the opposite trend (Fig. 4F-G). These findings implicated that SBF2-AS1 could regulate ESCC cell progression by targeting miR-494.

PFN2 was a target of miR-494

As predicted by starBase2.0, miR-494 comprised the binding sites of 3'UTR PFN2 (Fig. 5A). To disclose the functional role of PFN2, the expression of PFN2 mRNA and protein in ESCC tumors and cells was detected. As illustrated in Fig. 5B-D, PFN2 mRNA and protein levels were up-regulated in ESCC tumors compared with normal tissues. Up-regulation of PFN2 mRNA and protein expression was also discovered in ESCC cells in comparison with normal cells (Fig. 5E-F). Meanwhile, we noticed that miR-494 was negatively correlated with PFN2 (r=-0.605, $P<0.001$) (Fig. 5G). Importantly, luciferase activity was reduced in ESCC cells co-transfected with PFN2 3'UTR-WT and miR-494. However, there was no evident change

of luciferase activity in PFN2 3'UTR-MUT transfection group (Fig. 5H-I). In addition, miR-494 transfection repressed PFN2 protein expression in ESCC cells (Fig. 5J). Also, miR-494 inhibitor rescued SBF2-AS1 silencing-induced repression on PFN2 protein expression (Fig. 5K-L). All the data revealed that PFN2 was negatively regulated by miR-494 in ESCC.

Restoration of PFN2 rescued inhibition on cell proliferation, migration, invasion and EMT induced by SBF2-AS1 silencing in ESCC

Subsequently, the rescue experiments were conducted by transfecting sh-NC, sh-SBF2-AS1, sh-SBF2-AS1+pcDNA and sh-SBF2-AS1+PFN2 in Eca-109 and KYSE-150 cells. Apparently, PFN2 protein expression was promoted by PFN2 transfection (Fig. 6A). MTT results indicated that PFN2 counteracted the suppression on cell proliferation induced by SBF2-AS1 silencing (Fig. 6B-C). Simultaneously, cell migration and invasion were decreased by SBF2-AS1 silencing. However, PFN2 reversed the effects (Fig. 6D-E). Moreover, the production of protein MMP9 and Vimentin was blocked by SBF2-AS1 silencing and boosted by restoration of PFN2. By contrast, the expression of E-cadherin displayed the opposite trend (Fig. 6F-G). Altogether, SBF2-AS1 accelerated cell proliferation, migration, invasion and EMT in ESCC cells by enhancing PFN2.

Illustration of the association between SBF2-AS1/miR-494/PFN2 axis and ESCC cell progression

We illustrated the interrelation between SBF2-AS1/miR-494/PFN2 axis and ESCC cell

proliferation, migration, invasion and EMT. SBF2-AS1 could repress miR-494 to enhance PFN2 expression and further facilitating EMT by boosting MMP9, Vimentin protein expression and blocking E-cadherin protein expression. Hence, SBF2-AS1 was able to accelerate ESCC cell proliferation, migration and invasion by promoting EMT through regulating miR-494/PFN2 axis (Figure 7).

DISCUSSION

Growing evidences demonstrated that SBF2-AS1 was critical therapeutic biomarker in cancers, such as lung adenocarcinoma and hepatocellular carcinoma (R. Chen et al., 2019; Y. T. Zhang et al., 2018). Differentially expression of SBF2-AS1 was implicated in the growth of cancer cells. For instance, increased expression of SBF2-AS1 expedited cell development by repressing miR-140-5p and facilitating TGFBR1 expression in hepatocellular carcinoma (Y. Li et al., 2018). Likewise, SBF2-AS1 was up-regulated in non-small cell lung cancer, and overexpression of SBF2-AS1 initiated cell migration, invasion and impaired apoptosis (Lv et al., 2016). Specifically, up-regulation of SBF2-AS1 was reported to facilitate cell survival in ESCC cells (Chen et al., 2018). In addition, exosomal transfer of SBF2-AS1 was reported to improve chemo-resistance of temozolomide against glioblastoma (Z. Zhang et al., 2019). Whether SBF2-AS1 functioned as oncogene to improve malignancy in ESCC requires further exploration.

Based on the prediction by LncBase Predicted v.2, we discovered that SBF2-AS1 could specifically bind to miR-494. Hence, we assumed that SBF2-AS1 regulated cell behavior by targeting miR-494. Previous studies indicated that dysregulation of miR-494 was implicated

in different cancers, including melanoma, bladder and gastric cancer (J. Li et al., 2019; Peng et al., 2018; Z. Tian et al., 2019). For instance, increased miR-494 expression enhanced cell progression and sorafenib resistance by regulating PTEN in hepatocellular carcinoma (Liu et al., 2015). Similarly, elevation of miR-494 facilitated non-small cell lung cancer cell proliferation, migration and repressed apoptosis by regulation of CASP2 (Q. Zhang et al., 2019). Conversely, miR-494 attenuated breast cancer cell progression by binding to CXCR4 via Wnt/β-catenin signaling (Song et al., 2015). Also, miR-494 suppressed oral cancer cell growth by blocking HOXA10 expression (Liborio-Kimura, Jung, & Chan, 2015). Furthermore, miR-494 enhanced gastric cancer cell sensitivity during TRAIL treatment via repressing surviving production (Xu et al., 2018). Therefore, SBF2-AS1 regulated cell development by targeting miR-494 in ESCC.

We firstly investigated the role of SBF2-AS1 by online tool GEPIA2 and qRT-PCR. Up-regulation of SBF2-AS1 expression was observed in ESCC tumors and cells. As expected, knockdown of SBF2-AS1 attenuated ESCC cell proliferation, migration, invasion and EMT, implicating the oncogenic role of SBF2-AS1. Luciferase reporter system confirmed the interaction between miR-494 and SBF2-AS1 or PFN2. At the same time, we discovered that the expression of miR-494 was down-regulated, whereas PFN2 was up-regulated in ESCC tumors and cells compared with normal ones. Next, the molecular mechanism of ESCC cell progression was further investigated by rescue experiment. MiR-494 inhibitor alleviated SBF2-AS1 silencing-induced suppression on ESCC cell proliferation, migration, invasion and EMT. Consistently, restoration of PFN2 inversed the inhibition on cell proliferation, migration, invasion and EMT in ESCC induced by SBF2-AS1 silencing. In short, SBF2-AS1

accelerated cell proliferation, migration and invasion in ESCC by facilitating EMT through miR-494/PFN2 axis.

CONCLUSION

In conclusion, we clarified the specific molecular mechanism of SBF2-AS1 in ESCC tumorigenesis and progression. We discovered that SBF2-AS1 positively accelerated cell proliferation, migration, invasion and EMT in ESCC cells by sponging miR-494 and up-regulating PFN2 expression. Our study was capable of representing novel targeted methods for ESCC therapy.

Declaration of Interests

The authors have no interests to disclose.

Author contributions

Conceptualization: Qiu Zhang and Xixiang Pan; Investigation: Qiu Zhang and Dongyang You; Writing - original draft: Qiu Zhang and Xixiang Pan; Writing - review & editing: Qiu Zhang and Xixiang Pan; Supervision: Dongyang You.

References

Chen, G., Gu, Y., Han, P., Li, Z., Zhao, J. L. and Gao, M. Z. (2019). Long noncoding RNA SBF2-AS1 promotes colorectal cancer proliferation and invasion by inhibiting miR-619-5p activity and facilitating HDAC3 expression. *J. Cell. Physiol.* **234**, 18688-18696. doi:10.1002/jcp.28509

Chen, L., Yang, H., Yi, Z., Jiang, L., Li, Y., Han, Q., Yang, Y., Zhang, Q., Yang, Z., Kuang, Y., et al. (2019). LncRNA GAS5 regulates redox balance and dysregulates the cell cycle and apoptosis in malignant melanoma cells. *J. Cancer Res. Clin. Oncol.* **145**, 637-652. doi:10.1007/s00432-018-2820-4

Chen, R., Xia, W., Wang, S., Xu, Y., Ma, Z., Xu, W., Zhang, E., Wang, J., Fang, T., Zhang, Q. a., et al. (2019). Long noncoding RNA SBF2-AS1 is critical for tumorigenesis of early-stage lung adenocarcinoma. *Mol Ther Nucleic Acids* **16**, 543-553. doi:10.1016/j.omtn.2019.04.004

Chen, R., Xia, W., Wang, X., Qiu, M., Yin, R., Wang, S., Xi, X., Wang, J., Xu, Y., Dong, G., et al. (2018). Upregulated long non-coding RNA SBF2-AS1 promotes proliferation in esophageal squamous cell carcinoma. *Oncol Lett* **15**, 5071-5080. doi:10.3892/ol.2018.7968

Cheng, L., Kong, B., Zhao, Y. and Jiang, J. (2018). miR-494 inhibits cervical cancer cell proliferation through upregulation of SOCS6 expression. *Oncol Lett* **15**, 3075-3080. doi:10.3892/ol.2017.7651

Cui, X.B., Zhang, S.M., Xu, Y.X., Dang, H.W., Liu, C.X., Wang, L.H., Yang, L., Hu, J.M., Liang, W.H., Jiang, J.F., et al. (2016). PFN2, a novel marker of unfavorable prognosis, is a potential therapeutic target involved in esophageal squamous cell carcinoma. *J Transl Med* **14**, 137-137. doi:10.1186/s12967-016-0884-y

Gao, Z. Q., Wang, J. F., Chen, D. H., Ma, X. S., Yang, W., Zhe, T., and Dang, X. W. (2018). Long non-coding RNA GAS5 antagonizes the chemoresistance of pancreatic cancer cells through down-regulation of miR-181c-5p. *Biomed. Pharmacother.* **97**, 809-817. doi: 10.1016/j.biopha.2017.10.157

Guo, W., Liu, S., Dong, Z., Guo, Y., Ding, C., Shen, S., Liang, J. and Shan, B. (2018). Aberrant methylation-mediated silencing of lncRNA CTC-276P9.1 is associated with malignant progression of esophageal squamous cell carcinoma. *Clin. Exp. Metastasis* **35**, 53-68. doi:10.1007/s10585-018-9881-2

Hong, L., Chen, W., Wu, D. and Wang, Y. (2018). Upregulation of SNHG3 expression associated with poor prognosis and enhances malignant progression of ovarian cancer. *Cancer Biomark* **22**, 367-374. doi:10.3233/CBM-170710

Hou, G., Zhao, Q., Zhang, M., Fan, T., Liu, M., Shi, X., Ren, Y., Wang, Y., Zhou, J. and Lu, Z. (2018). Down-regulation of Rictor enhances cell sensitivity to PI3K inhibitor LY294002 by blocking mTORC2-medicated phosphorylation of Akt/PRAS40 in esophageal squamous cell carcinoma. *Biomed. Pharmacother.* **106**, 1348-1356. doi:10.1016/j.biopha.2018.07.075

Hu, X., Ding, D., Zhang, J. and Cui, J. (2019). Knockdown of lncRNA HOTAIR sensitizes breast cancer cells to ionizing radiation through activating miR-218. *Biosci. Rep.* **39**, doi:10.1042/BSR20181038

Jeong, D. H., Choi, Y. N., Seo, T. W., Lee, J. S. and Yoo, S. J. (2018). Ubiquitin-proteasome dependent regulation of Profilin2 (Pfn2) by a cellular inhibitor of apoptotic protein 1 (cIAP1). *Biochem. Biophys. Res. Commun.* **506**, 423-428. doi:10.1016/j.bbrc.2018.10.115

Kang, M., Ren, M., Li, Y., Fu, Y., Deng, M. and Li, C. (2018). Exosome-mediated transfer of lncRNA PART1 induces gefitinib resistance in esophageal squamous cell carcinoma via functioning as a competing endogenous RNA. *J. Exp. Clin. Cancer Res.* **37**, 171. doi:10.1186/s13046-018-0845-9

Kawaguchi, T., Komatsu, S., Ichikawa, D., Hirajima, S., Nishimura, Y., Konishi, H., Shiozaki, A., Fujiwara, H., Okamoto, K., Tsuda, H., et al. (2017). Overexpression of TRIM44 is related to invasive potential and malignant outcomes in esophageal squamous cell carcinoma. *Tumour Biol.* **39**, 1010428317700409. doi:10.1177/1010428317700409

Li, J., Chen, J., Wang, S., Li, P., Zheng, C., Zhou, X., Tao, Y., Chen, X., Sun, L., Wang, A., et al. (2019). Blockage of transferred exosome-shuttled miR-494 inhibits melanoma growth and metastasis. *J. Cell. Physiol.* doi:10.1002/jcp.28234

Li, N., Zhao, X., Wang, L., Zhang, S., Cui, M. and He, J. (2016). miR-494 suppresses tumor growth of epithelial ovarian carcinoma by targeting IGF1R. *Tumour Biol.* **37**, 7767-7776. doi:10.1007/s13277-015-4603-8

Li, Y., Liu, G., Li, X., Dong, H., Xiao, W. and Lu, S. (2018). Long non-coding RNA SBF2-AS1 promotes hepatocellular carcinoma progression through regulation of miR-140-5p-TGFBR1 pathway. *Biochem. Biophys. Res. Commun.* **503**, 2826-2832. doi:10.1016/j.bbrc.2018.08.047

Liborio-Kimura, T. N., Jung, H. M. and Chan, E. K. (2015). miR-494 represses HOXA10 expression and inhibits cell proliferation in oral cancer. *Oral Oncol.* **51**, 151-157. doi:10.1016/j.oraloncology.2014.11.019

Liu, K., Liu, S., Zhang, W., Jia, B., Tan, L., Jin, Z. and Liu, Y. (2015). miR-494 promotes cell proliferation, migration and invasion, and increased sorafenib resistance in hepatocellular carcinoma by targeting PTEN. *Oncol. Rep.* **34**, 1003-1010. doi:10.3892/or.2015.4030

Lv, J., Qiu, M., Xia, W., Liu, C., Xu, Y., Wang, J., Leng, X., Huang, S., Zhu, R., Zhao, M., et al. (2016). High expression of long non-coding RNA SBF2-AS1 promotes proliferation in non-small cell lung cancer. *J. Exp. Clin. Cancer Res.* **35**, 75-75. doi:10.1186/s13046-016-0352-9

Nishiumi, S., Fujigaki, S., Kobayashi, T., Kojima, T., Ito, Y., Daiko, H., Kato, K., Shoji, H., Kodama, Y., Honda, K., et al. (2019). Metabolomics-based discovery of serum biomarkers to predict the side-effects of neoadjuvant chemoradiotherapy for esophageal squamous cell carcinoma. *Anticancer Res.* **39**, 519-526. doi:10.21873/anticanres.13143

Peng, Q.P., Du, D.B., Ming, Q., Hu, F., Wu, Z.B. and Qiu, S. (2018). MicroRNA 494 increases chemosensitivity to doxorubicin in gastric cancer cells by targeting phosphodiesterases 4D. *Cell. Mol. Biol. (Noisy-le-grand)* **64**, 62-66. PMID: 30672438

Rong, X., Gao, W., Yang, X., and Guo, J. (2019). Downregulation of hsa_circ_0007534 restricts the proliferation and invasion of cervical cancer through regulating miR-498/BMI-1 signaling. *Life Sci.* **235**, 116785. doi:10.1016/j.lfs.2019.116785

Song, L., Liu, D., Wang, B., He, J., Zhang, S., Dai, Z., Ma, X. and Wang, X. (2015). miR-494 suppresses the progression of breast cancer in vitro by targeting CXCR4 through the Wnt/β-catenin signaling pathway. *Oncol. Rep.* **34**, 525-531. doi:10.3892/or.2015.3965

Tian, Y. J., Wang, Y. H., Xiao, A. J., Li, P. L., Guo, J., Wang, T. J. and Zhao, D. J. (2019). Long noncoding RNA SBF2-AS1 act as a ceRNA to modulate cell proliferation via binding with miR-188-5p in acute myeloid leukemia. *Artif Cells Nanomed Biotechnol* **47**, 1730-1737. doi:10.1080/21691401.2019.1608221

Tian, Z., Luo, Y., Zhu, J., Hua, X., Xu, J., Huang, C., Jin, H., Huang, H. and Huang, C. (2019). Transcriptionally elevation of miR-494 by new ChlA-F compound via a HuR/JunB axis inhibits human bladder cancer cell invasion. *Biochim Biophys Acta Gene Regul Mech* **1862**, 822-833. doi:10.1016/j.bbagrm.2019.05.007

VanGuilder, H. D., Vrana, K. E., and Freeman, W. M. (2008). Twenty-five years of quantitative PCR for gene expression analysis. *Biotechniques.* **44**, 619-626. doi:10.2144/000112776

Wang, H., Wu, W., Wang, H. W., Wang, S., Chen, Y., Zhang, X., Yang, J., Zhao, S., Ding, H. F., and Lu, D. (2010). Analysis of specialized DNA polymerases expression in human gliomas: association with prognostic significance. *Neuro-oncology.* **12**, 679-686. doi:10.1093/neuonc/nop074

Wu, Y., Xie, Z., Chen, J., Chen, J., Ni, W., Ma, Y., Huang, K., Wang, G., Wang, J., Ma, J., et al. (2019). Circular RNA circTADA2A promotes osteosarcoma progression and metastasis by sponging miR-203a-3p and regulating CREB3 expression. *Mol. Cancer.* **18**, 73. doi:10.1186/s12943-019-1007-1

Wu, Y., Yang, Y. and Xian, Y. S. (2019). HCRP1 inhibits cell proliferation and invasion and promotes chemosensitivity in esophageal squamous cell carcinoma. *Chem. Biol. Interact.* **308**, 357-363. doi:10.1016/j.cbi.2019.05.032

Xia, W., Liu, Y., Cheng, T., Xu, T., Dong, M. and Hu, X. (2020). Down-regulated lncRNA SBF2-AS1 inhibits tumorigenesis and progression of breast cancer by sponging microRNA-143 and repressing RRS1. *J. Exp. Clin. Cancer Res.* **39**, 18. doi:10.1186/s13046-020-1520-5

Xu, S., Li, D., Li, T., Qiao, L., Li, K., Guo, L. and Liu, Y. (2018). miR-494 sensitizes gastric cancer cells to TRAIL treatment through downregulation of survivin. *Cell. Physiol. Biochem.* **51**, 2212-2223. doi:10.1159/000495867

Zhang, J., Zhu, Y., Hu, L., Yan, F. and Chen, J. (2019). miR-494 induces EndMT and promotes the development of HCC (Hepatocellular Carcinoma) by targeting SIRT3/TGF-beta/SMAD signaling pathway. *Sci Rep* **9**, 7213. doi:10.1038/s41598-019-43731-4

Zhang, Q., Li, Y., Zhao, M., Lin, H., Wang, W., Li, D., Cui, W., Zhou, C., Zhong, J. and Huang, C. (2019). MiR-494 acts as a tumor promoter by targeting CASP2 in non-small cell lung cancer. *Sci Rep* **9**, 3008. doi:10.1038/s41598-019-39453-2

Zhang, Y., Li, Y., Han, L., Zhang, P. and Sun, S. (2019). SBF2-AS1: An oncogenic lncRNA in small-cell lung cancer. *J. Cell. Biochem.* **120**, 15422-15428. doi:10.1002/jcb.28809

Zhang, Y. T., Li, B. P., Zhang, B., Ma, P., Wu, Q. L., Ming, L. and Xie, L. M. (2018). LncRNA SBF2-AS1 promotes hepatocellular carcinoma metastasis by regulating EMT and predicts unfavorable prognosis. *Eur Rev Med Pharmacol Sci* **22**, 6333-6341. doi:10.26355/eurrev_201810_16044

Zhang, Z., Yin, J., Lu, C., Wei, Y., Zeng, A. and You, Y. (2019). Exosomal transfer of long non-coding RNA SBF2-AS1 enhances chemoresistance to temozolomide in glioblastoma. *J. Exp. Clin. Cancer Res.* **38**, 166. doi:10.1186/s13046-019-1139-6

Zhou, J., Zhang, S., Chen, Z., He, Z., Xu, Y., and Li, Z. (2019). CircRNA-ENO1 promoted glycolysis and tumor progression in lung adenocarcinoma through upregulating its host gene ENO1. *Cell. Death Dis.* **10**, 885. doi:10.1038/s41419-019-2127-7
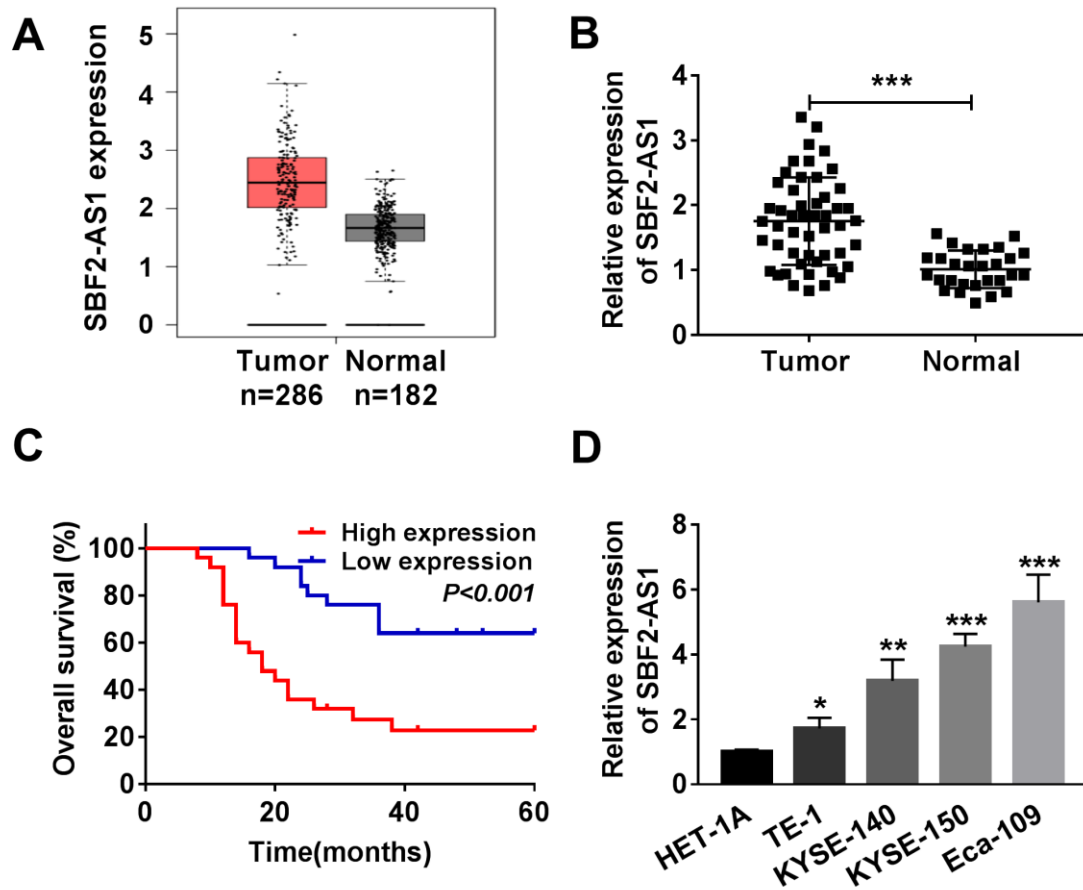
Figures

Fig. 1 SBF2-AS1 was up-regulated in ESCC. (A-B) SBF2-AS1 expression in ESCC tumors and normal tissues was analyzed by GEPIA2 and qRT-PCR. (C) Analysis of the overall survival rate in ESCC patients with high and low level of SBF2-AS1 was conducted. (D) SBF2-AS1 expression in ESCC cell lines (TE-1, KYSE-140, KYSE-150 and Eca-109) and human esophageal epithelium immortalized cells HET-1A was measured by qRT-PCR. *P<0.05, **P<0.01, ***P<0.001.
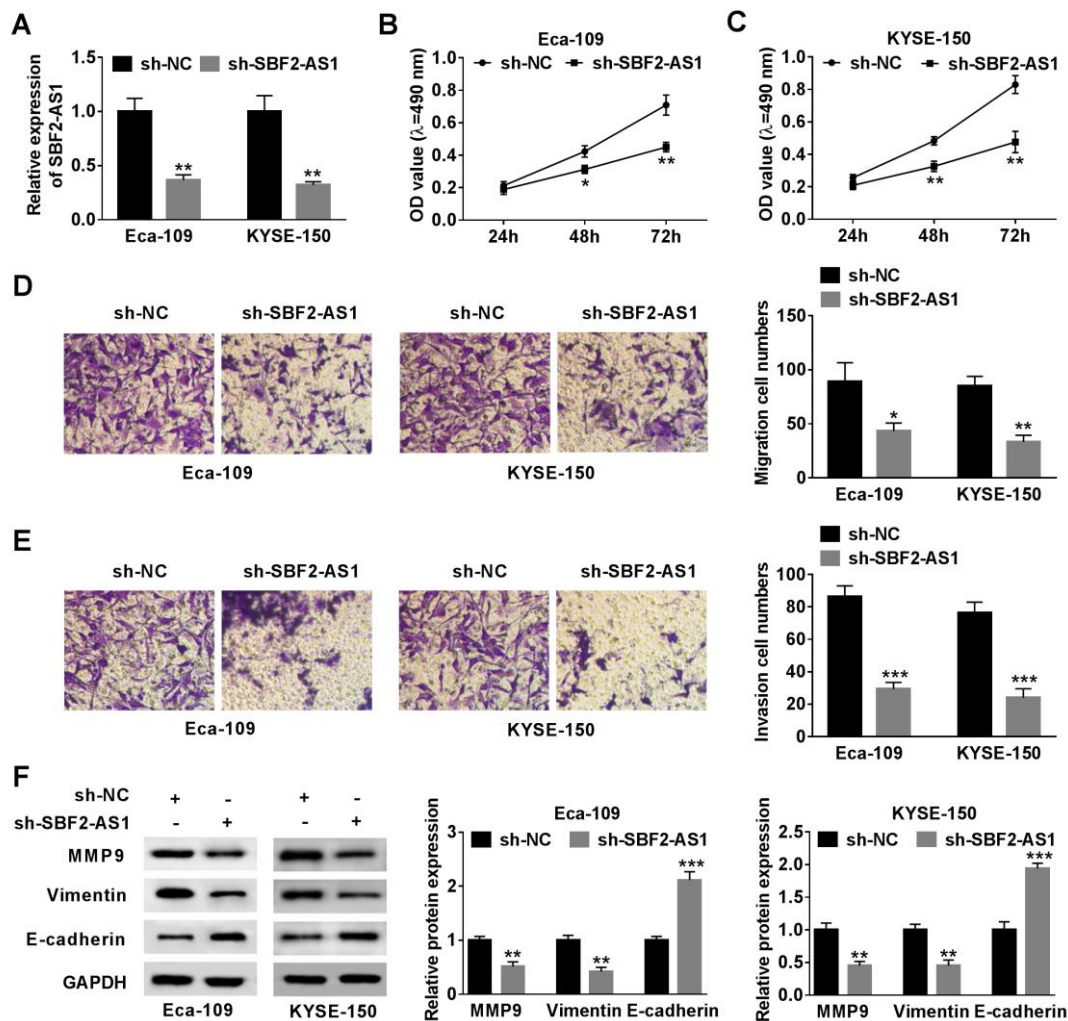
Fig. 2 SBF2-AS1 knockdown inhibited cell proliferation, migration, invasion and EMT in ESCC cells. Eca-109 and KYSE-150 cells were stably transfected with sh-SBF2-AS1 or sh-NC. (A) SBF2-AS1 expression in transfected Eca-109 and KYSE-150 cells was measured by qRT-PCR. (B-C) Cell viability of transfected Eca-109 and KYSE-150 cells was measured by MTT assay. (D-E) Cell migration and invasion of transfected Eca-109 and KYSE-150 cells were determined by transwell assay. (F) Protein expression of MMP9, Vimentin and E-cadherin in transfected cells was assessed by western blot. GAPDH was used as internal reference. $*P<0.05$, $**P<0.01$, $***P<0.001$.
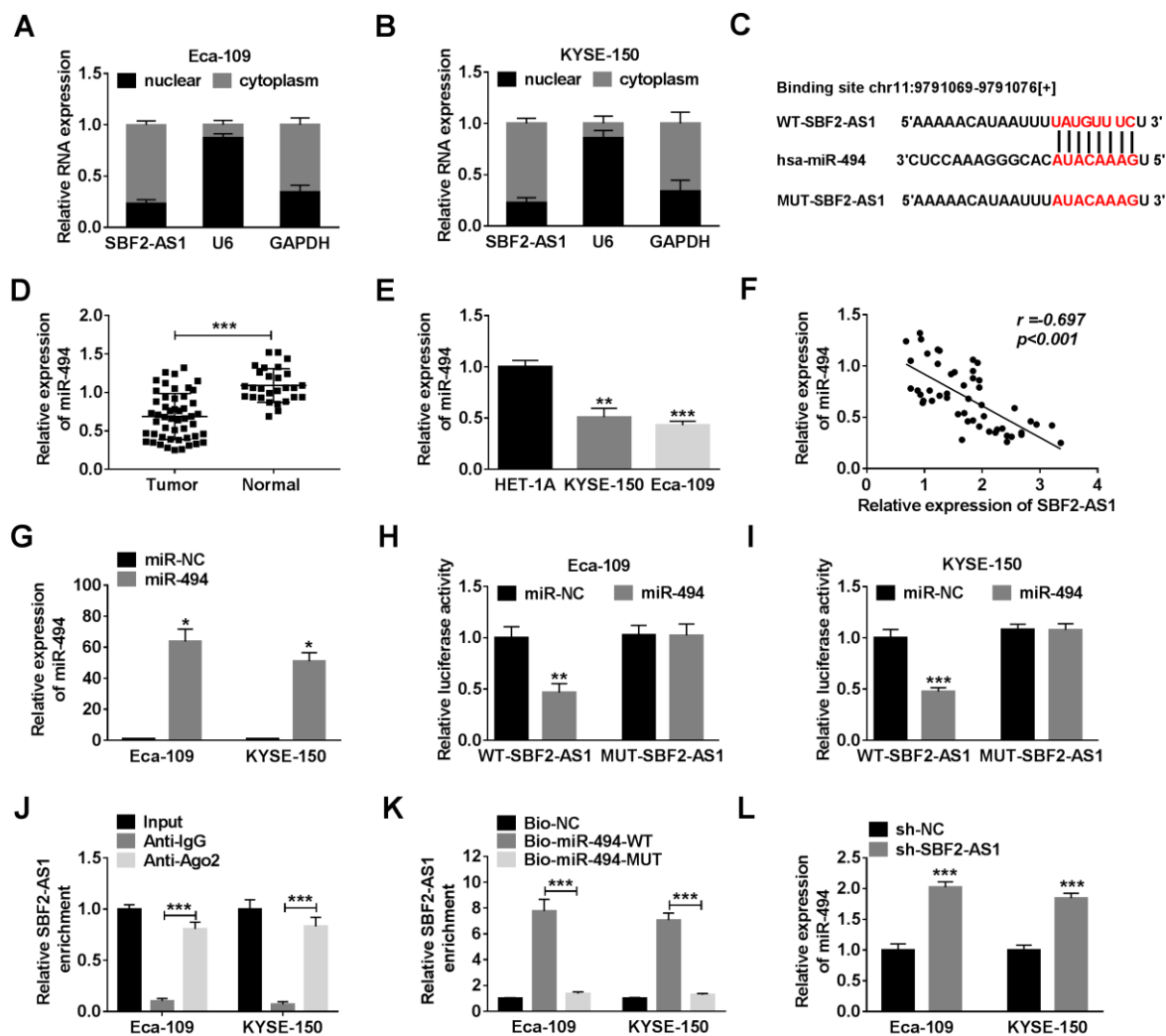
Fig. 3 SBF2-AS1 directly interacted with miR-494. (A-B) The expression of SBF2-AS1, U6 and GAPDH in the nuclear and cytoplasm isolated from Eca-109 and KYSE-150 cells was measured by qRT-PCR. (C) The putative binding sites between SBF2-AS1 and miR-494 were predicted by LncBase Predicted v.2. (D) The expression of miR-494 in ESCC tumors and normal tissues was measured by qRT-PCR. (E) The expression of miR-494 in Eca-109, KYSE-150 and HET-1A cells was measured by qRT-PCR. (F) Analysis of the correlation between SBF2-AS1 and miR-494 was conducted (r=-0.67, *P*<0.001). (G) The expression of miR-494 in Eca-109 and KYSE-150 cells transfected with miR-494 and miR-NC. (H-I)

Luciferase activity of Eca-109 and KYSE-150 cells co-transfected with WT-SBF2-AS1 or MUT-SBF2-AS1 and miR-494 or miR-NC was examined using luciferase reporter assay. (J) SBF2-AS1 enrichment in Eca-109 and KYSE-150 cells was examined by RIP assay. (K) SBF2-AS1 enrichment in Eca-109 and KYSE-150 cells transfected with Bio-NC, Bio-miR-494-WT and Bio-miR-494-MUT was detected by RNA pull-down assay. (L) The expression of miR-494 in Eca-109 and KYSE-150 cells stably transfected with sh-SBF2-AS1 and sh-NC was measured by qRT-PCR. *$P<0.05$, **$P<0.01$, ***$P<0.001$.
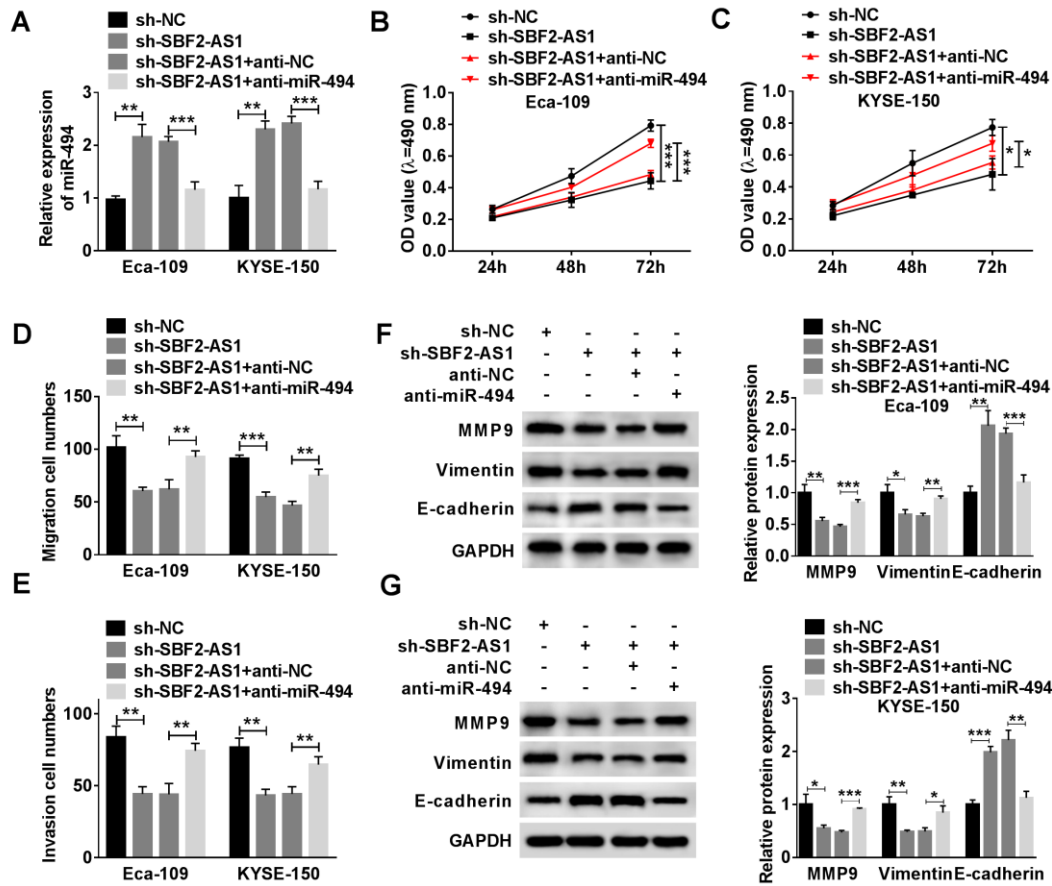
Fig. 4 MiR-494 inhibitor restored SBF2-AS1 silencing-mediated inhibition of cell proliferation, migration, invasion and EMT in ESCC. Eca-109 and KYSE-150 cells were transfected with sh-NC, sh-SBF2-AS1, sh-SBF2-AS1+anti-NC and sh-SBF2-AS1+anti-miR-494. (A) The expression of miR-494 in transfected Eca-109 and KYSE-150 cells was measured by qRT-PCR. (B-C) MTT assay was used to detect cell viability of transfected Eca-109 and KYSE-150 cells. (D-E) Cell migration and invasion of transfected Eca-109 and KYSE-150 cells were measured by transwell assay. (F-G) Western blot was applied to analyze protein expression of MMP9, Vimentin and E-cadherin in transfected Eca-109 and KYSE-150 cells. GAPDH was used as internal reference. $*P<0.05$, $**P<0.01$, $***P<0.001$.
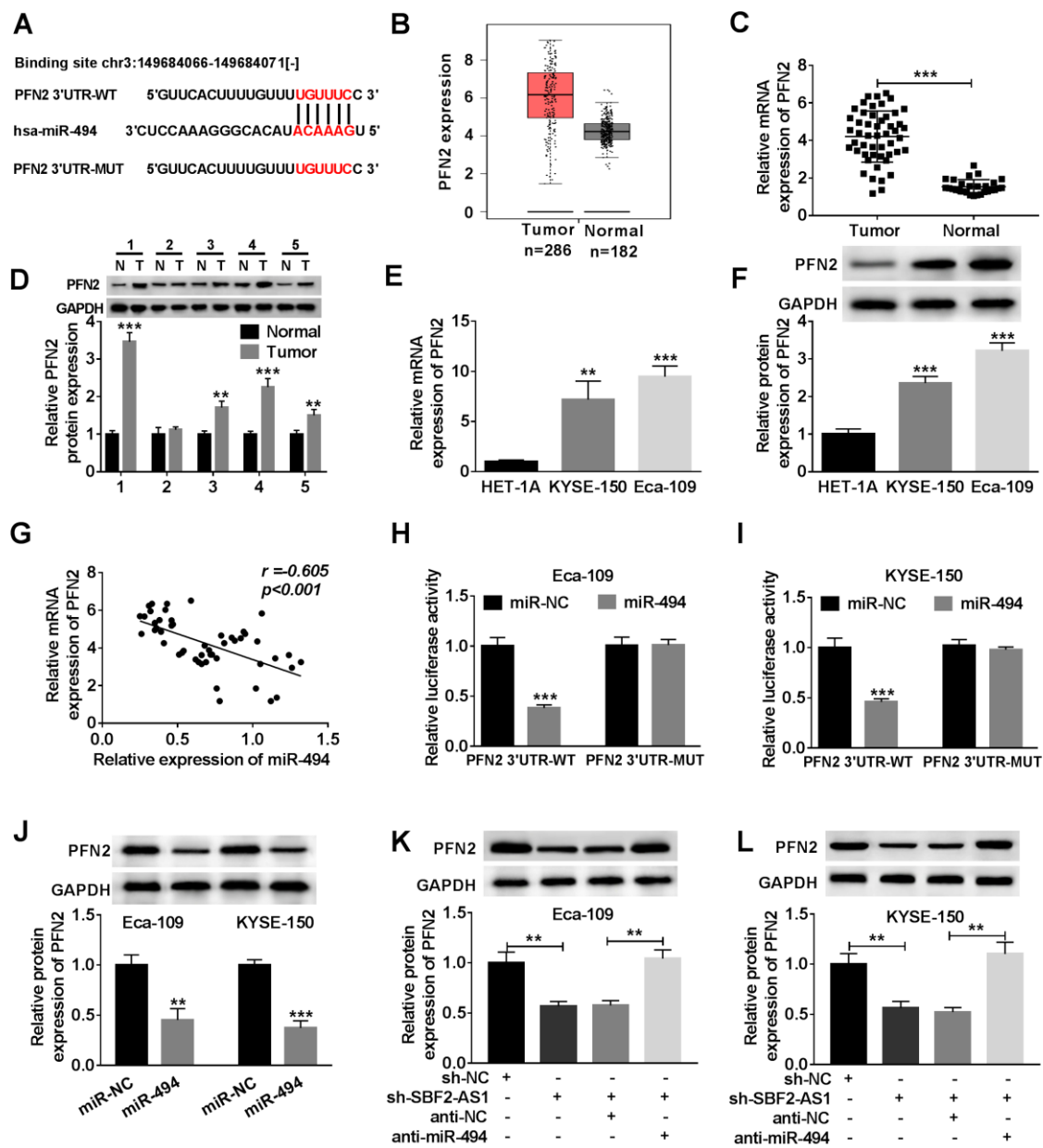
Fig. 5 PFN2 was a target of miR-494. (A) The putative binding sites between PFN2 and miR-494 predicted by starBase2.0. (B-D) PFN2 mRNA and protein expression in ESCC tumors and normal tissues were evaluated by GEPIA2, qRT-PCR and western blot, respectively. (E-F) The mRNA and protein expression of PFN2 in Eca-109, KYSE-150 and HET-1A cells were evaluated. (G) The correlation between miR-494 and PFN2 was analyzed (r=-0.605, *P*<0.001). (H-I) Luciferase activity of Eca-109 and KYSE-150 cells co-transfected

with PFN2 3'UTR-WT or PFN2 3'UTR-MUT and miR-494 or miR-NC was evaluated by luciferase reporter assay. (J) PFN2 protein expression in Eca-109 and KYSE-150 cells transfected with miR-494 or miR-NC was assessed by western blot. (K-L) PFN2 protein expression in Eca-109 and KYSE-150 cells transfected with sh-NC, sh-SBF2-AS1, sh-SBF2-AS1+anti-NC and sh-SBF2-AS1+anti-miR-494 was analyzed. **$P<0.01$, ***$P<0.001$.
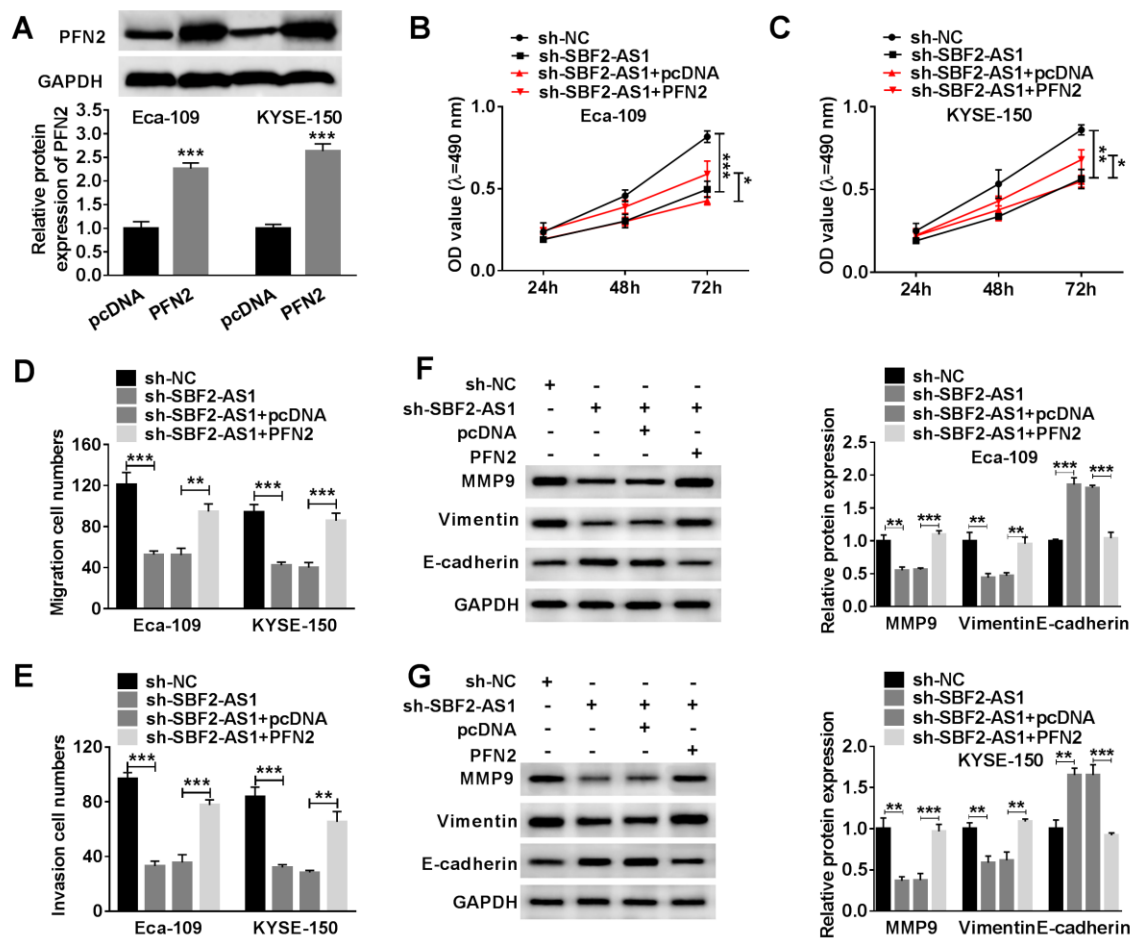
Fig. 6 PFN2 abrogated SBF2-AS1 silencing-mediated inhibition on cell proliferation, migration, invasion and EMT in ESCC. Eca-109 and KYSE-150 cells were stably transfected with sh-NC, sh-SBF2-AS1, sh-SBF2-AS1+pcDNA and sh-SBF2-AS1+PFN2. (A) PFN2 protein expression in transfected Eca-109 and KYSE-150 cells was examined by qRT-PCR. (B-C) Cell viability of transfected Eca-109 and KYSE-150 cells was detected by MTT assay. (D-E) Cell migration and invasion of transfected Eca-109 and KYSE-150 cells were measured by transwell assay. (F-G) Protein expression of MMP9, Vimentin and E-cadherin in transfected Eca-109 and KYSE-150 cells was evaluated by western blot. GAPDH was used as internal reference. *$P<0.05$, **$P<0.01$, ***$P<0.001$.
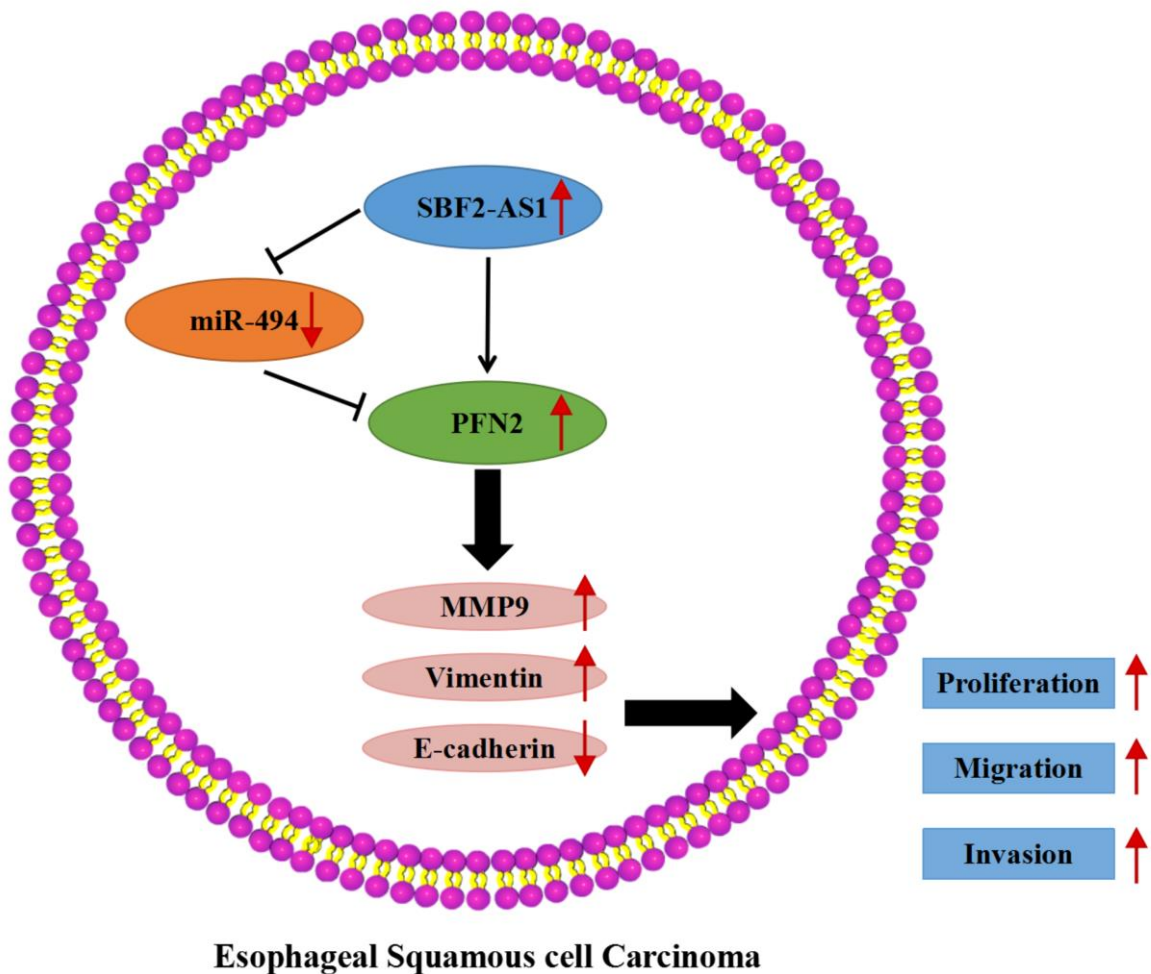
Esophageal Squamous cell Carcinoma

Fig. 7 The interrelation of SBF2-AS1/miR-494/PFN2 axis and cell proliferation, migration, invasion and EMT in ESCC was illustrated.

Supplement Table 1: Primers sequences

Name	Primer	Tm(°C)	Product size (bp)
SBF2-AS1	F: CACGACCCAGAAGGAGTCTAC R: CCCGGTACCTTCCTGTCATA	60	144
GAPDH	F: GCACCGTCAAGGCTGAGAAC R: GCCTTCTCCATGGTGGTGAA	60	226
PFN2	F: CGAGTCTCGTGGGCTACAAGGACTCG R: CAACCAGGACACCCACCTCAG	60	134
U6	F: GCTTCGGCAGCACATATACTAAAAT R: CGCTTCACGAATTTGCGTGTCAT	60	60
miR-494	F: GGAGAGGTTGTCCGTGTTGT R: AGGTTTCCCGTGTATGTTTCA	60	70